

Local eigenstates and parametric excitations of a simple atom-molecule Bose-Einstein condensate

Marijan Koštrun and Juha Javanainen

*Department of Physics, University of Connecticut, Storrs, Connecticut 06269-3046 **

(Dated: March 2, 2022)

Abstract

We model an atom-molecule Bose-Einstein condensate (AMBEC) using simplified set of coupled Gross-Pitaevskii equations (GPE), where we neglect the background (elastic) scattering length of the atoms. We analyze the ground state numerically and analytically, and construct its twin state through transformation $\delta \rightarrow -\delta, K \rightarrow -K$. We find that the ground state is a collection of three local eigenstates: all-atom state, mixed (atom-molecule) state, and all-molecule state, while the twin state comprises of mixed state with tunable fraction of atoms including unity but excluding all-molecules. We find the analytic boundaries of the local eigenstates from the stability analysis of the underlying all-molecule and all-atom eigenstate. In the ground state we find either regular oscillations in size and fraction of both condensates, or shrinking of the atomic condensate that resembles the collapse. In the twin state we find rapid irregular disintegration of both condensates.

We contrast the properties of the mean-field parametric excitations found in AMBEC with the experimentally observed excitations of the BEC. We discuss some enticing possibilities for creation of atomic BEC of controllable half-width by performing the parameter sweep around the boundary.

PACS numbers: 03.75.F,05.30.J,34.50

*Electronic address: kostrun@phys.uconn.edu

I. INTRODUCTION

Bose-Einstein condensation (BEC) in weakly interacting atomic gases continues to be of considerable experimental and theoretical interest. BEC dynamics strongly depends on atom-atom interactions, which is quite accurately described by their s-wave scattering length a . It was argued [1–5] that BEC with $a < 0$ may collapse in finite time [6] resulting in a gas-liquid phase transition [7–9]. Controlling the collapse is one way of controlling the atom-atom interactions [4, 10–12]. As is known, atom-atom interactions can be manipulated through Feshbach resonances in magnetic field or through photo-association [13–16]. Either mechanism can be described as a coupling of atomic pair to a molecular dimer [17–19].

The dynamics of dilute atomic BEC can be described using the mean-field theory [20], in which the macroscopic condensate wave function $\Phi = \Phi(\mathbf{r})$ is a solution of a Gross-Pitaevskii equation (GPE),

$$i\hbar\frac{\partial\Phi(\mathbf{r},t)}{\partial t} = \left(-\frac{\hbar^2}{2m}\nabla^2 + V_0(\mathbf{r},t)\right)\Phi(\mathbf{r},t) + \frac{4\pi\hbar^2aN}{m}|\Phi(\mathbf{r},t)|^2\Phi(\mathbf{r},t). \quad (1)$$

Here, we choose Φ normalized to unity with N being the number of atoms in the condensate, V_0 the trapping potential, while m is the mass of an atom and $a > 0$ atom-atom s-wave scattering length.

It has been recognized that the mean-field approach of Eq. (1) may fail in certain situations, however, the cause of failure is embedded in the mean-field equations themselves: E.g., so-called collapse of the condensate for $a \lesssim -0.67$ is a parametric excitation of Eq. (1) in which the (non-linear) eigenstate present and continuous for $a \gtrsim -0.67$ disappears. One can thus conjecture for single-species BEC that the mean-field approximation is likely to fail if it predicts parametric excitations of some sort. A renormalization of negative scattering length calls for coupled atomic and molecular dimer BEC, so their mean-field theory needs to be examined with respect to parametric excitations.

We build phenomenological mean-field theory of atom-molecule BEC (AMBEC) from three parameters: K , coupling strength between a pair of atoms and a molecule, δ , the detuning of the molecular state[28], and the background atom-atom scattering length [21]. However, close to the resonance the atom-atom scattering length is dominated by the resonant contribution so there the background scattering length can be safely ignored. Their

Gross-Pitaevskii equations read,

$$i\frac{\partial\varphi}{\partial\tau} = H_a\varphi - K\varphi^*\psi, \quad (2a)$$

$$i\frac{\partial\psi}{\partial\tau} = (H_m - \delta)\psi - K\varphi^2. \quad (2b)$$

The Hamiltonians H_a and H_m correspond to the center-of-mass energies for atoms and molecules, respectively,

$$H_a = -\frac{1}{2}\nabla^2 + \frac{1}{2}\mathbf{r}^2, \quad (3a)$$

$$H_m = -\frac{1}{4}\nabla^2 + \mathbf{r}^2. \quad (3b)$$

For simplicity, we assume that both atomic and molecular trap are isotropic with the same trap frequency ω , which we then use to scale all the other frequencies. Similarly, we use characteristic length of the atomic trap $L_0 = \sqrt{\frac{\hbar}{m\omega}}$ to scale all the distances. Lastly, we scale the fields with respect to the total number of particles, so that the normalization reads

$$\langle\varphi|\varphi\rangle + \langle\psi|\psi\rangle = 1. \quad (4)$$

The expression for the conserved total energy of the system is then

$$E = \langle\varphi|H_a|\varphi\rangle + \frac{1}{2}\langle\psi|H_m - \delta|\psi\rangle + E_I, \quad (5)$$

where

$$E_I = -\frac{1}{2}K(\langle\varphi^2|\psi\rangle + \langle\psi|\varphi^2\rangle). \quad (6)$$

In this paper we examine two collections of eigenstates of AMBEC (2) that are symmetric with respect to the resonant detuning δ : the ground state and its “twin state.” We use zero-dimensional analysis to find the local eigenstates in parameter space, and examine their stability. We then extend analysis to the full mean-field AMBEC equations numerically and analytically. We find the extent of local eigenstates comprising each collection, and examine (i), their parametric excitations; and (ii), how in certain parametric sweeps the same excitations can be avoided.

II. ZERO-DIMENSIONAL AMBEC

For zero-dimensional analysis, we assume free condensates, which are described by plane waves of varying amplitudes [15, 21, 22]. We absorb all the constants in $\delta \leftarrow \delta/K$, so the

atomic $\alpha = \alpha(t)$ and the molecular $\beta = \beta(t)$ amplitude are the solutions of

$$i\dot{\alpha} = -\alpha^*\beta, \quad (7a)$$

$$i\dot{\beta} = -\delta\beta - \alpha^2. \quad (7b)$$

We expand time dependency of the amplitudes as $\alpha = x \cdot \exp(-i\mu t)$ and $\beta = y \cdot \exp(-i2\mu t)$, with x and y real, and normalize them so that $x^2 + y^2 \equiv 1$.

We find the stationary solutions of Eq. (7) as:

- The all-molecule state:

$$y \equiv \pm 1, \quad (8)$$

which exists for $\forall \delta$, and with $\mu = -\delta/2$.

- The mixed atom-molecule states:

$$y^{(-)}(\delta) = \frac{\delta}{6} + \frac{\sqrt{\delta^2 + 12}}{6}, \quad (9)$$

which exists for $\delta \leq 2$, and

$$y^{(+)}(\delta) = \frac{\delta}{6} - \frac{\sqrt{\delta^2 + 12}}{6}, \quad (10)$$

which exists for $\delta \geq -2$.

For both mixed states we have $\mu^{(\pm)} = -y^{(\pm)}$.

In Fig. 1 we show $\mu = \mu(\delta)$ for all stationary solutions.

To examine their stability we rewrite Eq. (7) in terms of the positive molecular amplitude $y = |\beta|$, and the phase difference $\theta = 2 \arg(\alpha) - \arg(\beta)$,

$$\dot{y} = (1 - y^2) \sin \theta, \quad (11a)$$

$$\dot{\theta} = \delta + \left(\frac{1}{y} - 3y \right) \cos \theta. \quad (11b)$$

The stationary solutions have $\theta = 0$ or π . The all-molecule state $y \equiv 1$ can have either θ . The two mixed atom-molecule states are given for $\theta = 0$ by $y^{(-)}$ from Eq. (9), and for $\theta = \pi$ by $-y^{(+)}$ from Eq. (10). We find the frequency of small oscillations λ near the stationary states $y^{(\pm)}$ as,

$$\lambda^2 = \cos^2 \theta (1 - y^2) \left(\frac{1}{y^2} + 3 \right), \quad (12)$$

which is always non-negative. We thus conclude that the mixed states are stable.

The all-molecule state we find stable everywhere except for $|\delta| < 2$, cf. [22]. In the limit $|\delta| \gg 1$ we find $\theta \approx \delta \cdot t$, while $\delta y(t) = 1 - y(t)$ behaves as,

$$\delta y(t) \approx \delta y(0) \cdot \exp \left[-\frac{\sqrt{2}}{\delta} (1 - \cos(\delta \cdot t)) \right]. \quad (13)$$

Thus, in the limit $t \rightarrow \infty$ small oscillations between atoms and molecules persist and do not die out.

From the all-molecule and the mixed states we construct the ground state around $\theta = 0$, and which exists for $\forall \delta$: $y_{GS} = y^{(-)}$ for $\delta < 2$, and $y_{GS} = 1$ for $\delta > 2$. We construct the second eigenstate around $\theta = \pi$, which we call the twin state: $y_{TW} = y^{(+)}$ for $\delta > -2$, and $y_{TW} = -1$ for $\delta < -2$. One can see that the twin state is symmetric to the ground state with respect to $\delta \rightarrow -\delta$ and $y \rightarrow -y$. We remark that $\delta = \pm 2$ are the critical points where the mixed state coincides with the all-molecule state but the transition is non-smooth: In parameter sweeps these points act as a source of parametric excitations.

III. NUMERICAL INVESTIGATION

We turn to numerical methods [23] to find the AMBEC (2) ground state and examine the properties of the underlying stationary states, the ground state and the twin state, by parameter sweeps in K and δ directions. For compactness of presentation, in our calculations we limit ourselves to spherically symmetric trap, that is, the atomic and molecular Hamiltonians contain only radial operators.

A. Ground State

We find the ground state through numerical iteration in complex time, followed by renormalization. We focus on the integer mesh $\delta = -30 \dots 30$, and $K = 0.1, 1 \dots 30$, where we use $K = 0.1$ as an approximation of the limit $K \rightarrow 0$. For each pair (δ, K) we find the condensate wave functions of atoms φ , and of molecules ψ . We present features of the atomic condensate in terms of its fraction $N_a = \langle \varphi | \varphi \rangle$, and the half-size $R_{1/2}$,

$$\frac{\int_0^{R_{1/2}} dr r^2 |\varphi(r)|^2}{\int_0^\infty dr r^2 |\varphi(r)|^2} = \frac{1}{2}. \quad (14)$$

N_a and $R_{1/2}$ calculated for the ground state that we show in Figs. 2 and 3 strongly suggest that the ground state comprises three local eigen-states: mostly-atom state, mixed atom-molecule state, and the all-molecule state. We surmise the existence of two boundaries, one f_{GS}^1 , between the mostly-atom and mixed state, and the other f_{GS}^2 , between the all-molecules and the mixed state.

We confirm presence of the boundaries f_{GS}^1 and f_{GS}^2 through parametric sweeps: They act as a source of parametric excitations.

Firstly, in Fig. 4 we show that the sweep of $K = 0 \dots 18$ for fixed $\delta = -30$ reveals a parametric excitation near $K = 17$, which we associate with f_{GS}^1 .

Secondly, in Fig. 5 we show that the sweep of $\delta = -30 \dots 30$ for fixed $K = 10$ reveals a parametric excitation near $\delta = 8$, which we associate with f_{GS}^2 . Interestingly, for $\delta < 0$ we do not see the evidence of f_{GS}^1 .

We address the differences between excitations at f_{GS}^1 and f_{GS}^2 in Sec. V, when we present our analytic treatment of the boundaries.

B. Twin State

Based on the zero-dimensional model, the twin state is an all-atom state for $\delta > 0$. We create it by adiabatically evolving an all-atom state found for $\delta > 0$ and $K \equiv 0$, to desired value of K . We demonstrate the effectiveness of this technique in Fig. 6, where we start from an all-atom state and sweep $K = 0 \dots 36$ for fixed $\delta = 100$. This also demonstrates that the twin state is not fully symmetric with the ground state as an equivalent of the boundary f_{GS}^1 that would be constructed by changing the sign of δ , is missing.

However, in parameter sweep in $\delta = 50 \dots -30$ for fixed $K = 10$, which we show in Fig. 7, we do find parametric excitations near $\delta = -3$. This suggests presence of the boundary f_{TW} , which is analogous to f_{GS}^2 .

IV. ANALYTIC TREATMENT OF THE BOUNDARIES

A. Boundary f_{GS}^1 and the extent of the all-atom state

We start by recalling that in the limit $K \rightarrow 0$ and $-\delta \gg K$, we can write the approximate solution of AMBEC(2) for mean-field ψ as, $\psi \simeq -\frac{K}{\delta}\varphi^2$. This then appears in the atomic GPE (1) as a tunable atom-atom s-wave scattering length $a_f = \frac{K^2}{4\pi\delta} < 0$. In the literature, it is known that atomic BEC can exist with small negative a_f . When this a_f is manipulated (increased in absolute value) to the critical value $a_f \rightarrow -0.67$ the atomic BEC collapses.

The expression for the effective scattering length a_f above is singular near $\delta = 0$. We now show how singularities can be removed under the assumption that both mean-fields are stationary. We start by writing the equation for ψ in AMBEC,

$$\left(i\frac{\partial}{\partial t} + \delta - H_m\right)\psi = -K\varphi^2, \quad (15)$$

In the limit in which the fraction of the atoms is much greater than the fraction of the molecules, $\langle\varphi|\varphi\rangle \gg \langle\psi|\psi\rangle$, the evolution of ψ is completely dominated by φ^2 . We assume that the eigen-energy is ϵ , so that the time dependence is $\varphi \sim e^{-i\epsilon t}$ and $\psi \sim e^{-i2\epsilon t}$, and that we can neglect other terms in expansion of ψ , that is, $H_m\psi \approx E_{0,m}\psi$, where $E_{0,m} = \langle\psi|H_m|\psi\rangle/\langle\psi|\psi\rangle$. Then, we can solve Eq. (15) for the mean-field ψ as,

$$\psi \approx -\frac{K}{2\epsilon + \delta - E_{0,m}}\varphi^2. \quad (16)$$

We can now use the atomic part of AMBEC(2) to write the equation for ϵ as,

$$\epsilon = E_{0,a} + \frac{K^2}{2\epsilon + \delta - E_{0,m}} \cdot \frac{\langle\varphi^2|\varphi^2\rangle}{\langle\varphi|\varphi\rangle}. \quad (17)$$

Here we use $H_a\varphi \approx E_{0,a}\varphi$, where $E_{0,a} = \langle\varphi|H_a|\varphi\rangle/\langle\varphi|\varphi\rangle$, similarly to what we have done for the molecules. The two solutions of Eq. (17) are ϵ^\pm , where

$$\epsilon^\pm = \frac{1}{4}(2E_{0,a} + E_{0,m} - \delta) \pm \frac{1}{4}\sqrt{(2E_{0,a} - E_{0,m} + \delta)^2 + 8K^2\frac{\langle\varphi^2|\varphi^2\rangle}{\langle\varphi|\varphi\rangle}}. \quad (18)$$

where the negative branch corresponds to the ground state, while the positive branch to the twin state. We remark that ϵ^\pm in Eq. (18) are everywhere well behaved, and that ϵ^\pm differ in sign of $2\epsilon + \delta - E_{0,m}$.

We use variational technique [20, 21, 24] to find $\epsilon = \epsilon(s)$ for the all-atom state, $\langle \varphi | \varphi \rangle = 1$, where φ is given by

$$\varphi(r; s) = \frac{1}{(\pi s^2)^{3/4}} e^{-\frac{r^2}{2s^2}}. \quad (19)$$

The variational energies are

$$E_{0,a} = \frac{3(1+s^4)}{4s^2} = E_{0,m}, \quad (20a)$$

$$\langle \varphi^2 | \varphi^2 \rangle = \frac{1}{2\sqrt{2}\pi^{3/2}s^3}, \quad (20b)$$

which then enter the expression for ϵ , Eq. (18). We find roots of $\partial\epsilon/\partial s = 0$ that are real and positive, and determine which of them are local minima of $\epsilon(s)$. We keep in mind that $s \gtrsim 1$ is a signature of an all-atom state, while $s \ll 1$ of the mixed- or all-molecule state.

In Fig. 8 we show the variational size s as a function of δ and K for the negative branch of ϵ , which corresponds to the ground state. We see that for larger negative δ 's the boundary f_{GS}^1 of the all-atom state coincide with the expected $\frac{K^2}{4\pi\delta} \simeq -0.67$. However, for $K \lesssim 15$ the boundary disappears near $\delta \sim -10$, just as we have seen in the numerical simulations, cf. Fig. 5. The reason why is because by approaching the expected boundary the fraction of atoms N_a begins to decrease, and this modulates the coupling as $K \cdot N_a$. This effect is so small, however, that it is accessible only for small initial magnitudes of coupling K .

An equivalent analysis for the twin state is utterly un insightful: continuous variational solution exists in the entire parameter space. We thus turn our attention to the opposite limit - that of the all-molecule state.

B. Boundaries f_{GS}^2 and f_{TW} of the all-molecule state

1. Existence of variational solutions for the atoms

We examine stability of the all-molecule ground state in the presence of infinitesimal atomic configurations. The all-molecule state is the ground state of H_m ,

$$\psi(r) = \left(\frac{2}{\pi}\right)^{3/4} e^{-r^2}. \quad (21)$$

Its eigen-energy is easily found in the absence of atomic mean-field,

$$\mu = \frac{1}{2} \left(\frac{3}{2} - \delta \right). \quad (22)$$

The atomic mean-field small in fraction, $\langle\varphi|\varphi\rangle \ll 1$, is then described by,

$$\mu\varphi = H_a\varphi - K\varphi^*\psi, \quad (23)$$

where μ is given by Eq. (22). We now approximate the atomic mean-field with Eq. (19), and define difference $\lambda^{GS}(s)$, where

$$\lambda^{GS}(s) \langle\varphi|\varphi\rangle = \langle\varphi|H_a|\varphi\rangle - \mu - K\langle\varphi^2|\psi\rangle. \quad (24)$$

We notice that for (real) φ the atomic norm cancels out. Valid sizes for the atomic condensates s satisfy,

$$\lambda^{GS}(s) = 0. \quad (25)$$

We find that Eq. (25) has either two solutions for s (we write this as $\lambda^{GS} \gtrless 0$, that is, λ_{GS} is positive for some values of s and negative for the others), or has no solution ($\lambda^{GS}(s) > 0, \forall s$).

We identify as f_{GS}^2 the boundary between the two regions, for which s is a double root.

In Fig. 9 we show the boundary f_{GS}^2 in the parameter space.

For the twin state, the phase shift between the molecular amplitude ψ and the matrix element K is -1 , so the new difference λ^{TW} now reads,

$$\lambda^{TW} \langle\varphi|\varphi\rangle = \langle\varphi|H_a|\varphi\rangle - \mu + K\langle\varphi^2|\psi\rangle. \quad (26)$$

Again, valid sizes for the atomic condensates s satisfy,

$$\lambda^{TW}(s) = 0. \quad (27)$$

The rest of the analysis is identical to what we have done for the ground state. In Fig. 9 we combine the findings for the ground state ($K > 0$) and the twin state ($K < 0$). Here, we identify the boundary as f_{TW} .

In Table I we give f_{GS}^2 as K for various detunings δ , where K_{num} are the numerical values we find by solving the full AMBEC, while K_{var} are the variational solutions. For comparison, we also give numerical values for the fraction (N_a^{mix}) and the half-size ($R_{1/2}^{mix}$) of the atomic distribution on the mixed side (on the atomic side both values are near unity). From Table I we see that across f_{GS}^2 the size and the fraction of atomic condensate change discontinuously. The boundary thus acts as a source of parametric excitations for parameter sweeps crossing it.

We numerically examine f_{TW} through parameter sweeps of the twin state for $K = 10, 20$. In Table II we list the detunings at which the condensates disintegrate as δ_{num} and the fraction of atoms at the onset of the instability as N_a^{mix} . We see that the mixed state disintegrates very close to $\delta = 0$. In this region the effective scattering length is large positive number. The analysis of ϵ^+ suggests that at f_{TW} the variational size s of the atomic condensate is maximal.

We show how these traits are related to the stability of the all-molecule state.

2. Stability of the all-molecule state

We write the solution of Eq. (2a) in the form

$$\varphi(\tau) = (a(\tau) + i b(\tau)) \varphi(r; s) \exp(-i\mu\tau), \quad (28)$$

where $\varphi(r; s)$ is the unit-normalized variational atomic amplitude, Eq. (19), and μ is the eigen-energy of the all-molecule state, Eq. (22). The time dependent real functions satisfy $|a(\tau)| \ll 1$ and $|b(\tau)| \ll 1$. We integrate out the eigenstate φ to yield a system of ordinary differential equations,

$$\begin{aligned} \dot{a} &= (\langle\varphi|H_a|\varphi\rangle - \mu + K \langle\varphi^2|\psi\rangle) b, \\ \dot{b} &= -(\langle\varphi|H_a|\varphi\rangle - \mu - K \langle\varphi^2|\psi\rangle) a. \end{aligned} \quad (29)$$

The frequency λ of small excitations is given by,

$$\begin{aligned} \lambda^2(s) &= (\langle\varphi|H_a|\varphi\rangle - \mu)^2 - K^2 |\langle\varphi^2|\psi\rangle|^2 \\ &= \lambda^{GS}(s) \cdot \lambda^{TW}(s). \end{aligned} \quad (30)$$

Stability of the molecular mean-field ψ then requires that $\lambda^2(s) > 0, \forall s > 0$. Conversely, if $\exists s' > 0$ such that $\lambda^2(s') < 0$, then this particular atomic mean-field may grow in fraction exponentially, and so destroy the ‘‘all-molecule’’ character of the eigenstate. Interestingly, this also means that if the molecular mean-field is stable ($\lambda^2 > 0$) then there are no available variational solutions for the atomic mean-field (it requires $\lambda^{GS} = 0$ or $\lambda^{TW} = 0$), and *vice versa*. Unavailability of of the atomic configurations in the vicinity of all-molecule state has been hinted by the zero-dimensional AMBEC, where the same occurs, cf. Eq. (13)

We combine these findings in Fig. 10 where we show the stability regions of the all-molecule state. We identify three regions (I, II and III) separated by two boundaries, f_{TW} between I and II, and f_{GS}^2 between II and III. We conclude that the all-molecule state of

the ground state is stable only in Region III, while the twin state does not have stable all-molecule configurations.

C. Summary of AMBEC eigenstates

We construct the maps of the ground state and the twin state from the analysis of their two limiting configurations, all-atom and all-molecule, as follows:

- *Ground state:* In Fig. 11 we show the outline of the ground state proposed in this report. It comprises three stationary states: all-atom, mixed and all-molecule state. The three stationary states are separated by two boundaries, f_{GS}^2 (between the mixed state and the all-molecule state) and f_{GS}^1 (partially separates all-atoms from mixed). For large negative detunings f_{GS}^1 is given by the single GPE collapse boundary $\frac{K^2}{4\pi\delta} = -0.67$. The AMBEC(2) interprets the collapse as that by crossing f_{GS}^1 for large K by increasing δ , the size of atomic mean-field reduces drastically and discontinuously. This boundary, however, does not extend to the origin. So, at least in principle, it is possible to perform a parameter sweep around the boundary and produce controllably narrow atomic mean-field without parametric excitations.
- *Twin State:* We show its outline in Fig. 12. It comprises the all-atom state and the mixed state, and disappears in a region of parameter space between $\delta \simeq 0$ and f_{TW} .

V. DISCUSSION

We have studied the stationary states of the simple atom-molecule Bose-Einstein Condensate (AMBEC) numerically and analytically. We have shown that, while the ground state remains a global eigenstate, the twin state does not. Non-linearity of AMBEC equations implies that all stationary states need not be eigenstates: For that they also have to be stable under small perturbations. The boundaries of the stationary states are a likely source of parametric excitations in sweeps as across such a boundary the properties of the stationary state may change discontinuously.

In parametric sweeps we have seen two types of parametric excitations near the all-molecule stationary state. In the first one type, the fraction of the atomic condensate

remains small, while the size varies erratically. We saw that in the ground state near the boundary f_{GS}^2 . In the second type, the atomic condensate grows in fraction and in size erratically which in some regions of parameter space may resemble an explosion. This is what we see in the decay of the twin state near f_{TW} .

A parameter sweep that follows the twin state in parameter space, has been realized in the ‘‘Bosenova’’ experiments [4]. The excitations of the BEC in a near-resonant region, observed on that occasion, followed by the loss of the atomic condensate makes a tempting parallel to the chaotic behavior we are predicting. The AMBEC we have examined suggests that the decay occurs because we have created a system in a local eigenstate, and have swept the parameters out of the bounds in which the eigenstate exists. While the onset of parametric excitations is in the scope of the mean-field approach, analysis of its final products may require inclusion of quantum corrections [5, 25–27].

We have presented a way to calculate system energy even near resonance, where the standard expansions in δ fail. In addition, our result in the case of simple AMBEC hints an exciting possibility to create almost-all atom state of various sizes while avoiding the parametric excitation tied to a_{crit} of the all-atom state (as accessible in Feshbach resonance experiments). Interestingly, our findings suggest that the disintegration of the simple AMBEC twin state might be even more spectacular. Studies of a trapped AMBEC on the time scale of the trap, both experimental and theoretical, might have other such intriguing surprises in store.

Acknowledgments

This work is supported in part by NSF (PHY-0097974) and NASA (NAG8-1428).

-
- [1] F. Dalfovo and S. Stringari, Phys. Rev. A **53**, 2477 (1996).
 - [2] R. Duine and H. T. C. Stoof, Phys. Rev. Lett. **86** (2001).
 - [3] J. M. Gerton, D. Strekalov, I. Prodan, and R. G. Hulet, Nature **408**, 692 (2000).
 - [4] E. Donley, N. Claussen, S. Cornish, J. Roberts, E. Cornell, and C. Wieman, Nature **412**, 295 (2001).
 - [5] R. Duine and H. Stoof, J. Opt. B **5**, 212 (2003).

- [6] M. Wadati and T. Tsurumi, Phys. Lett. A **247**, 287 (1998).
- [7] H. Stoof, Phys. Rev. A **49**, 3824 (1994).
- [8] E. Timmermans, P. Tommasini, R. Côté, M. Hussein, and A. Kerman, Phys. Rev. Lett. **83**, 2691 (1999).
- [9] S. Koh, Phys. Rev. B **64**, 134529 (2001).
- [10] S. Cornish, N. Claussen, J. Roberts, E. Cornell, and C. Wieman, Phys. Rev. Lett. **85**, 1795 (2000).
- [11] S. Kokkelmans, J. Milstein, M. Chiofalo, R. Walser, and M. Holland, Phys. Rev. A **65**, 53617 (2002).
- [12] T. Weber, J. Herbig, M. Mark, H. Nagerl, and R. Grimm, Science **299**, 232 (2003).
- [13] P. O. Fedichev, Y. Kagan, G. V. Shlyapnikov, and J. T. M. Walraven, Phys. Rev. Lett. **77**, 2913 (1996).
- [14] J. Bohn and P. Julienne, Phys. Rev. A **60**, 414 (1999).
- [15] M. Koštrun, M. Mackie, R. Côté, and J. Javanainen, Phys. Rev. A **62**, 063616 (2000).
- [16] J. Roberts, N. Clausen, S. Cornish, E. Donley, E. Cornell, and C. Wieman, Phys. Rev. Lett. **86**, 4211 (2001).
- [17] P. Drummond, K. Kheruntsyan, and H. He, Phys. Rev. Lett. **81**, 3055 (1998).
- [18] J. Javanainen and M. Mackie, Phys. Rev. A **58**, R789 (1998).
- [19] D. Kaplan, M. Savage, and M. Wise, Nucl. Phys. B **478**, 629 (1996).
- [20] A. Parkins and D. Walls, Phys. Rep. **303**, 1 (1998).
- [21] E. Timmermans, P. Tommasini, M. Hussein, and A. Kerman, Phys. Rep. **315**, 199 (1999).
- [22] Y. Wu and R. Côté, Phys. Rev. A **65**, 053603 (2002).
- [23] M. Koštrun and J. Javanainen, J. Comp. Phys. **172**, 298 (2001).
- [24] F. Dalfovo, S. Giorgini, L. Pitaevskii, and S. Stringari, Rev. of Mod. Phys. **71**, 463 (1999).
- [25] M. Mackie, K.-A. Suominen, and J. Javanainen, Phys. Rev. Lett. **89**, 180403 (2002).
- [26] S. Kokkelmans and M. Holland, Phys. Rev. Lett. **89**, 180401 (2002).
- [27] T. Köhler, T. Gasenzer, and K. Burnett, Phys. Rev. A **67**, 013601 (2003).
- [28] Here the detuning δ is given by $\delta = \nu_1 - E_b/\hbar$, where ν_1 is the laser frequency and E_b the energy of the molecular state E_b . We choose this convention so that the sign of the effective atom-atom scattering length conveniently coincides with the sign of detuning.

Figures and Captions

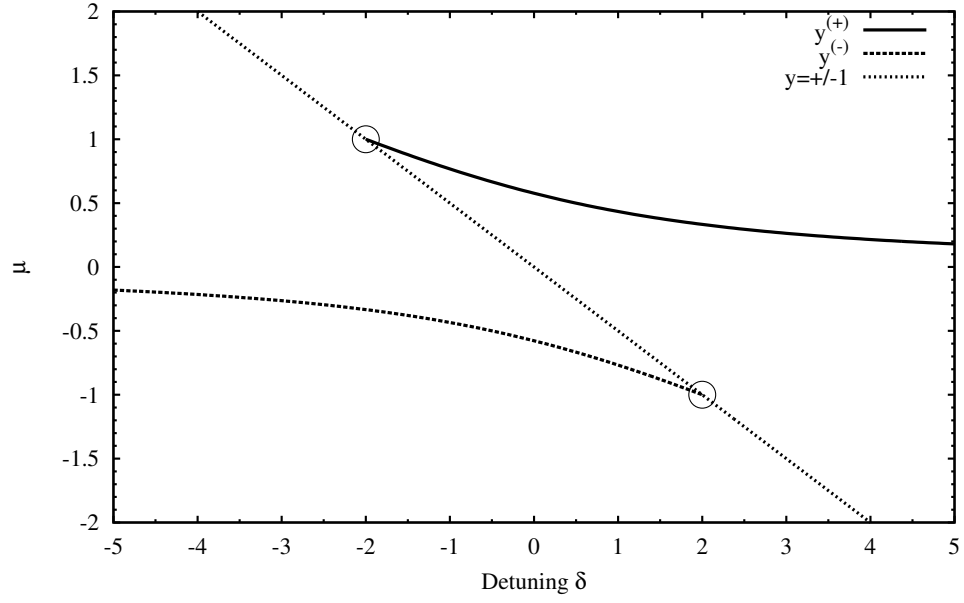


FIG. 1: Energy μ for the stationary states of Eq. (7), with the critical points $\delta = \pm 2$.

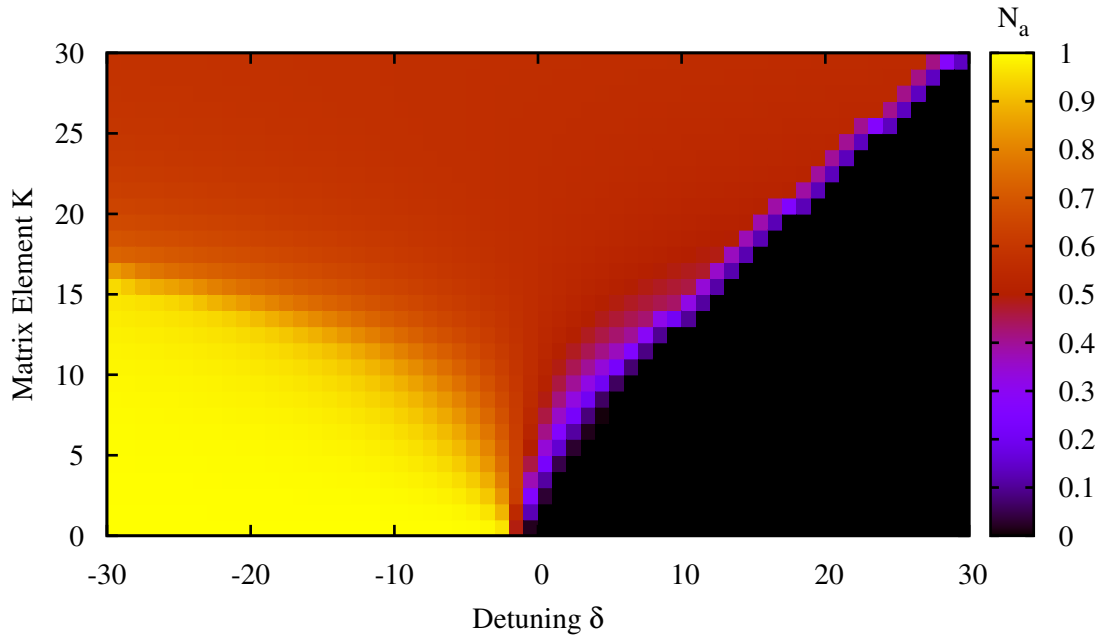


FIG. 2: (Ground state) Fraction of atoms (N_a) as a function of δ and K we find from evolution of GPEs (2) in complex time. One can easily recognize the regions of the mostly-atom state (in yellow, for $\delta < 0$) and the all-molecule state (in black, for $\delta > 0$).

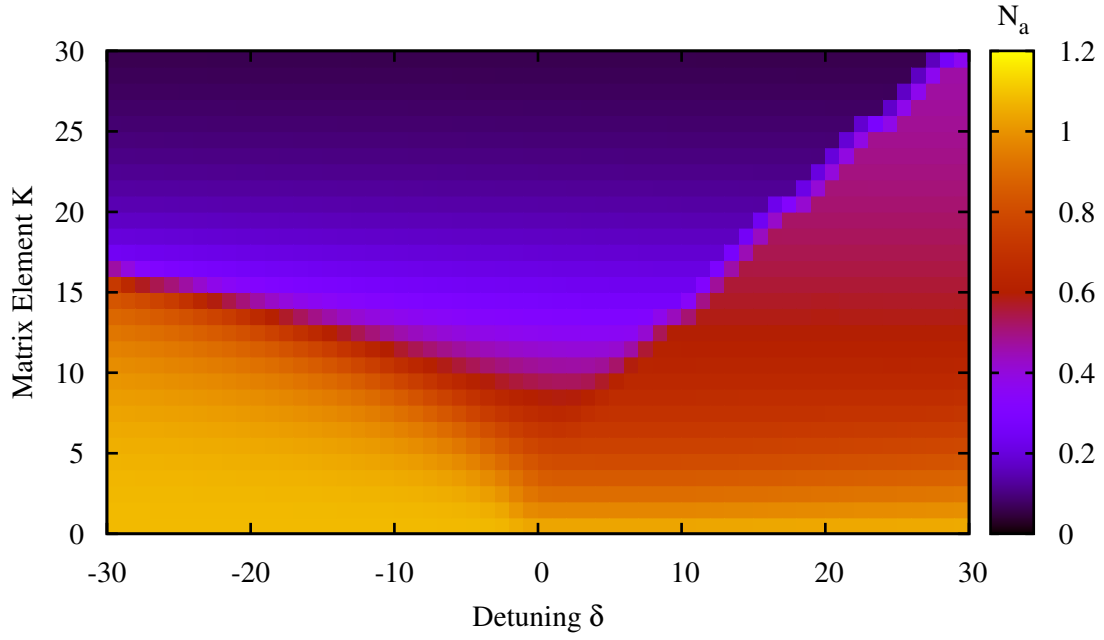


FIG. 3: (Ground state) $R_{1/2}$ as a function of δ and K we find from evolution of GPEs (2) in complex time. In the region of the mostly-atom state (cf. to Fig. 2, in yellow, for $\delta < 0$) we see the effects of the boundary f_{GS}^1 , where it separates the mostly-atom state of $R_{1/2} \simeq 1$ from a mixed state which atomic fraction is very narrow, $R_{1/2} \ll 1$.

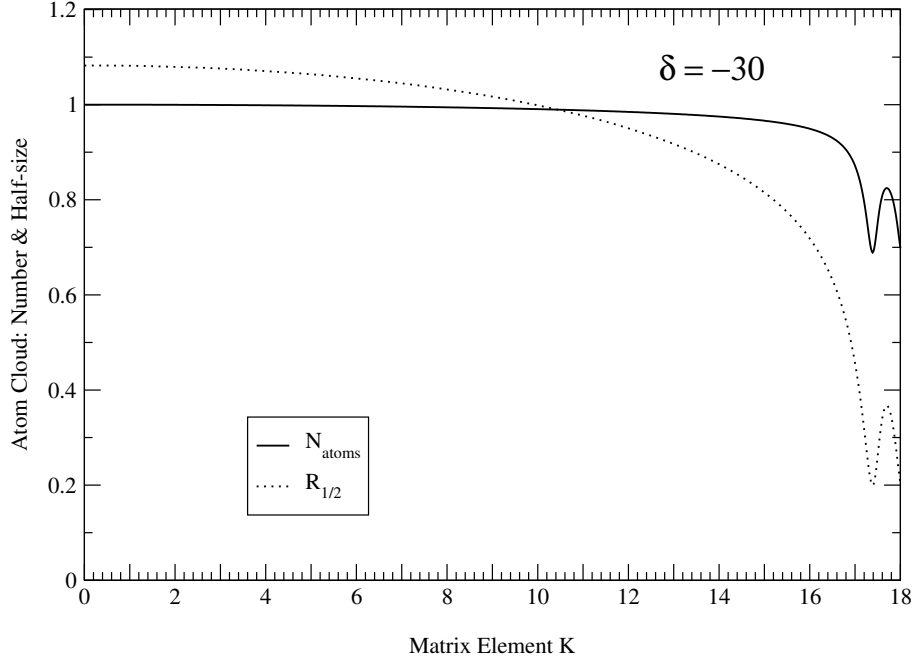


FIG. 4: (Ground state) N_a and $R_{1/2}$ in parameter sweep in $K = 0 \dots 18$ with fixed $\delta = -30$. Oscillations near $K = 17$ suggest a parametric excitation associated with crossing the boundary f_{GS}^1 .

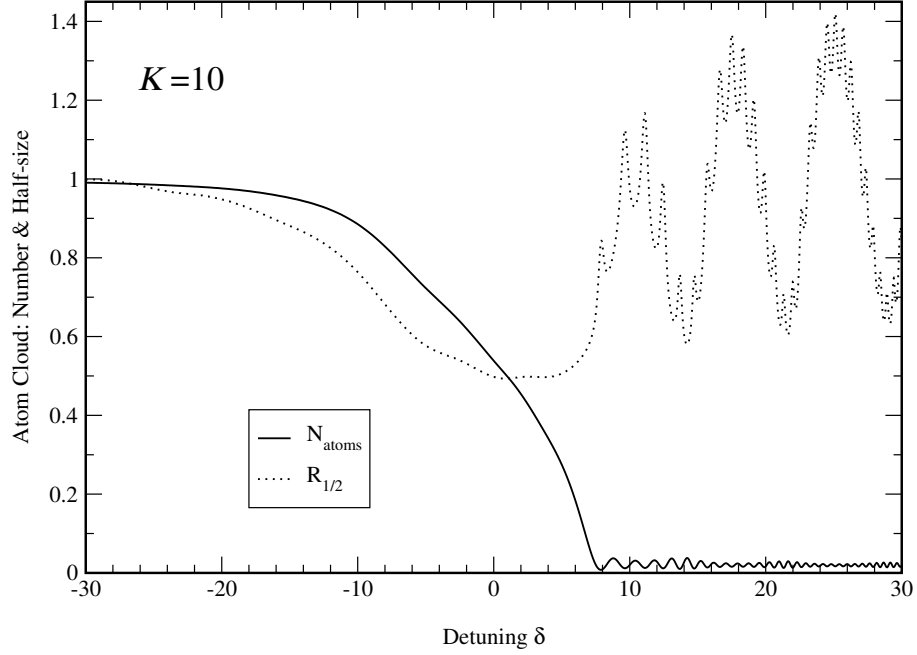


FIG. 5: (Ground state) N_a and $R_{1/2}$ in parameter sweep of $\delta = -30 \dots 30$ with $K = 10$ fixed. Oscillations near $\delta = 8$ suggest a parametric excitation from crossing the boundary f_{GS}^2 . Curiously, the anticipated oscillations from f_{GS}^1 near $\delta = 0$ are absent.

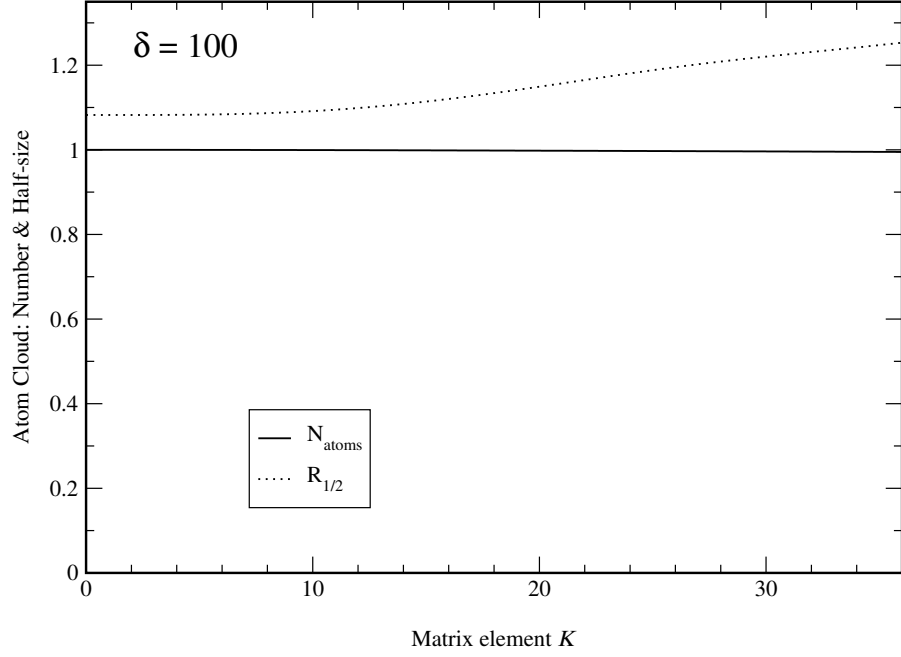


FIG. 6: (Twin state) Parametric sweep of $K = 0 \dots 36$ with fixed $\delta = 100$ of an all-atom state shows no evidence of parametric excitations. We use this technique to create the twin state at desired K and $\delta > 0$.

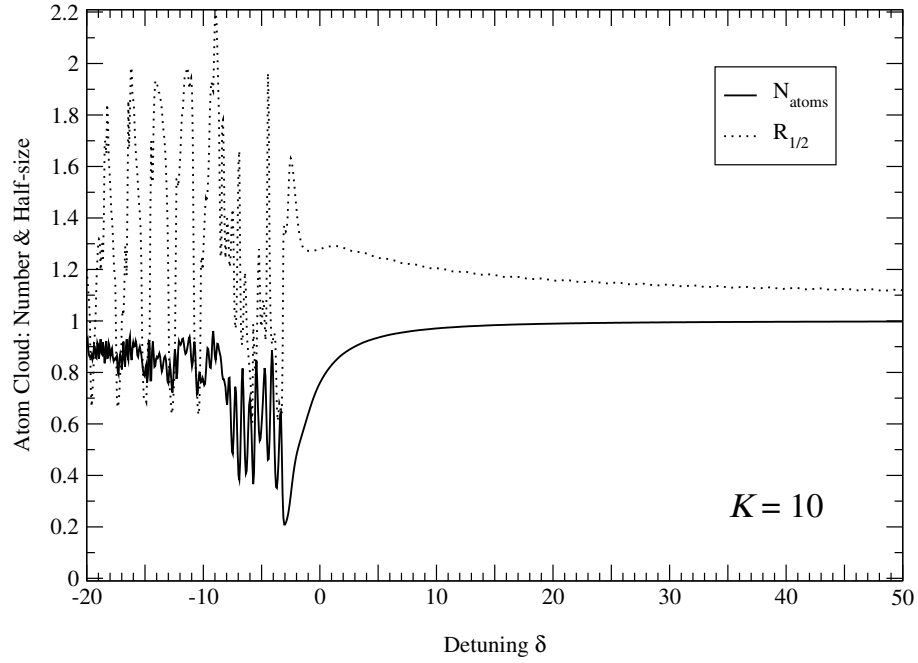


FIG. 7: Parametric sweep of all-atom state for $\delta = 50 \dots -30$ with $K = 10$ fixed reveals parametric excitation near $\delta = -3$.

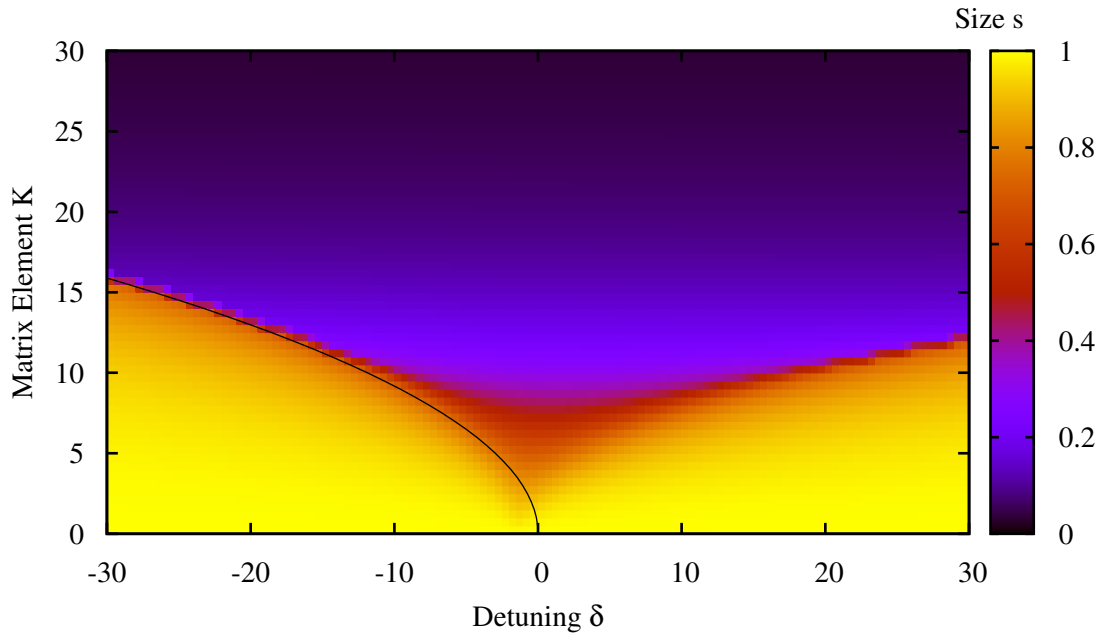


FIG. 8: The variational size of the atomic BEC in AMBEC as a function of detuning δ and matrix element K . For comparison the solid black line is the extent of the ground state in the pure atomic BEC, $K^2/(4\pi\delta) = -0.67$, and it coincides almost everywhere with f_{GS}^1 except near origin, where f_{GS}^1 disappears.

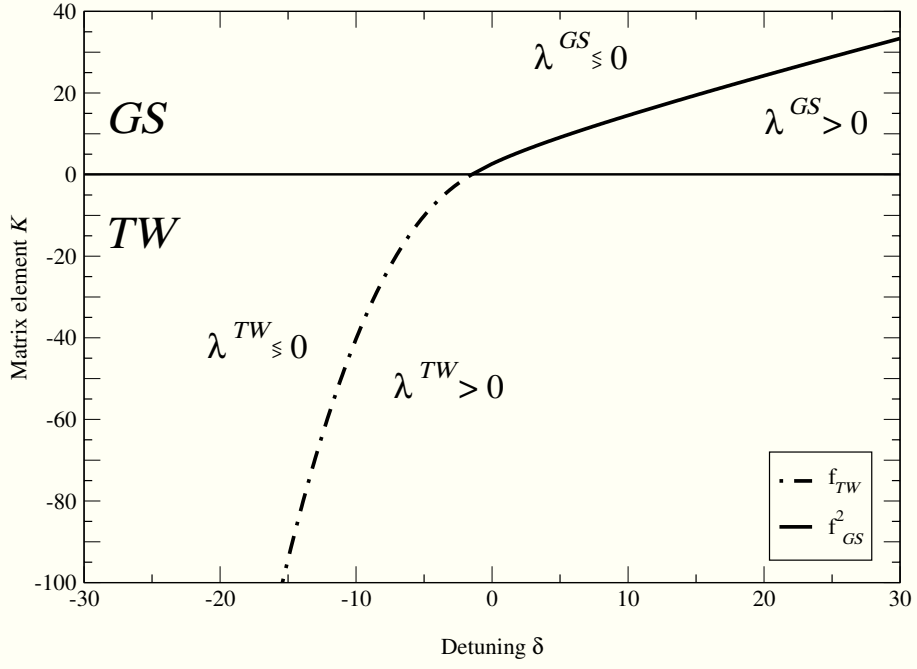


FIG. 9: Variational infinitesimal atomic configurations may exist only if Eq. (25) has real roots, which we write as $\lambda^{TW,GS} \gtrless 0$. As discussed in text, the case $K > 0$ pertains to the ground state, while $K < 0$ to the twin state. For $\lambda^{TW,GS} > 0$ there are no variational atomic configurations. The boundaries f_{TW} and f_{GS}^2 separate the regions with atomic configurations from the regions without.

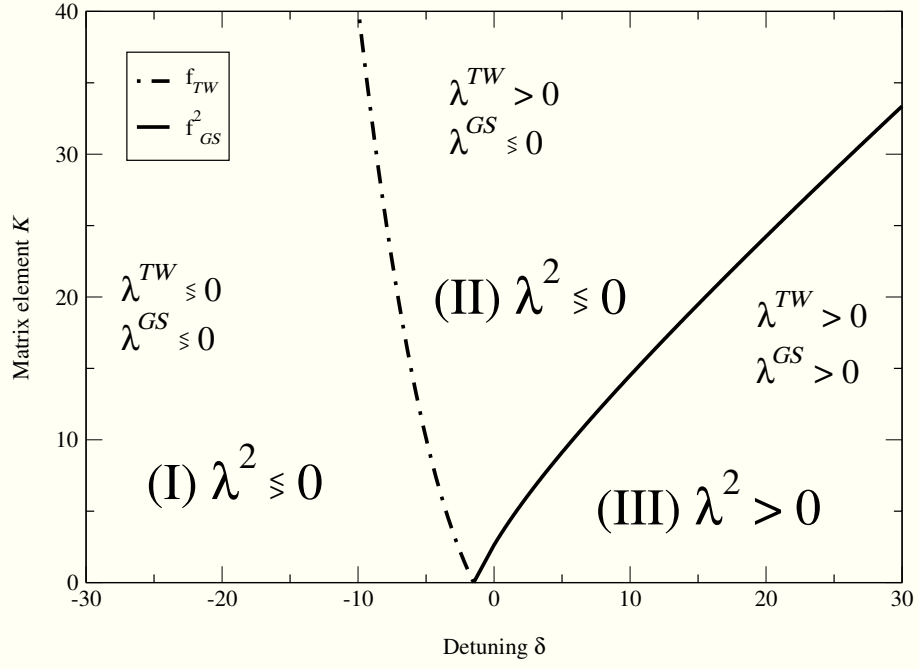


FIG. 10: Regions of λ^2 , Eq. (30), in the parameter space. λ^2 is positive only in Region III, bounded by f_{GS}^2 , for all variational atomic sizes s . In all other regions there exist unstable variational solutions for s , for which $\lambda^2 < 0$.

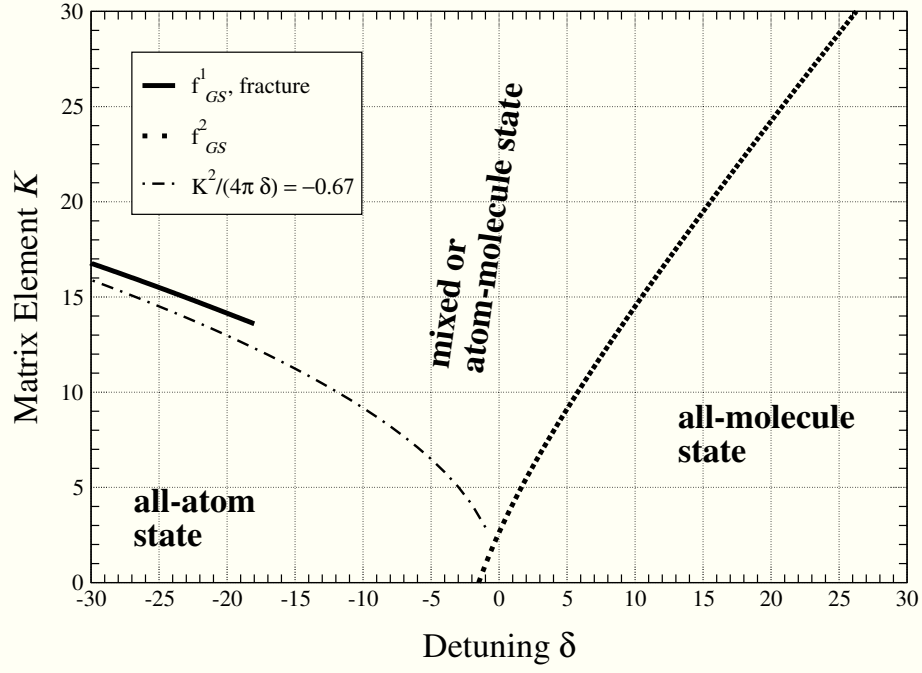


FIG. 11: Map of the ground state with the boundaries f^1_{GS} and f^2_{GS} separating the three local stationary states. Please note that f^1_{GS} only partially bounds the all atom state.

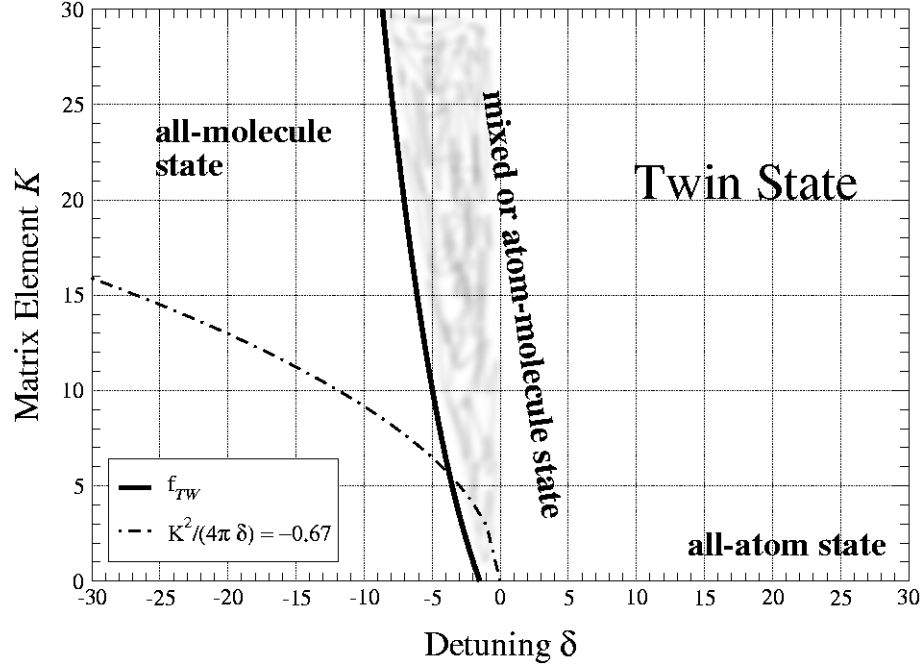


FIG. 12: Map of the twin state with the boundary f_{TW} separating the all-molecule state from the mixed state. The actual boundary of the twin state is somewhere in the shaded region.

Tables and Captions

δ	K_{var}	K_{num}	N_a^{mix}	$R_{1/2}^{mix}$
-1.5	0	0	-	-
0	2.6	2.5 ± 0.5	0.13	0.76
1	4.1	4.5 ± 0.5	0.18	0.76
5	9.1	9.5 ± 0.5	0.25	0.52
10	14.5	14.5 ± 0.5	0.42	0.28
20	24.2	24.5 ± 0.5	0.55	0.09
30	33.4	33.5 ± 0.5	0.66	0.03

TABLE I: Comparison of the variational and (full AMBEC) numerical results for the position of the boundary f_{GS}^2 in the format K for various δ . From numerical solutions we also extract the fraction of atoms N_A and the half-radius $R_{1/2}$ for the mixed state (superscript *mix*) at $K_{num} + 0.5$, on the all-atom side these are both unity.

δ_{var}	K	δ_{num}	N_a^{mix}
-1.5	0	-	-
-3.54	5	-	-
-4.98	10	-3.0	0.21
-7.07	20	-3.9	0.32
-8.66	30	-	-
-11.11	50	-	-
-15.42	100	-	-

TABLE II: Comparison of the variational and (full AMBEC) numerical results for the position of the boundary f_{TW} . In column N_a^{mix} we give the estimated fraction of atoms prior to disintegration of the condensates.